PCCP

PAPER

View Article Online
View Journal | View Issue

Cite this: *Phys. Chem. Chem. Phys.*, 2023, **25**, 6025

Synthesis of photocatalytic cysteine-capped $Cu_{\approx 10}$ clusters using Cu_5 clusters as catalysts†

Shahana Huseyinova,[a] José M. Blanco Trillo,[a] José M. Ramallo-López,[b] Félix G. Requejo,[b] David Buceta*[a] and M. Arturo López-Quintela*[a]

Received 3rd October 2022,
Accepted 10th January 2023

DOI: 10.1039/d2cp04550h

rsc.li/pccp

We report an easily scalable synthesis method for the preparation of cysteine-capped $Cu_{\approx 10}$ clusters through the reduction of Cu(II) ions with $NaBH_4$, using Cu_5 clusters as catalysts. The presence of such catalytic clusters allows controlling the formation of the larger $Cu_{\approx 10}$ clusters and prevents the production of copper oxides or Cu(I)–cysteine complexes, which are formed when Cu_5 is absent or at lower concentrations, respectively. These results indicate that small catalytic clusters could be involved, as precursor species before the reduction step, in the different methods developed for the synthesis of clusters. The visible light-absorbing $Cu_{\approx 10}$ clusters, obtained by the cluster-catalysed method, display high photocatalytic activities for the decomposition of methyl orange with visible light.

1. Introduction

Metal clusters represent one of most exciting examples of the novel properties that can be found at the bottom of the nanoscale.[1–5] Due to their small size there is a strong quantum confinement of the free electrons introducing a splitting at the Fermi level. The discretization of the energy levels implies that clusters can be viewed as atomic-scale semiconductors, with increasing band gap as cluster size decreases.[6–8] Metal clusters have been applied in the last decade mainly as fluorescence sensors (cluster-dots)[1,2] but also in catalysis,[9–11] photocatalysis,[12–14] *etc.* However, the main challenge is to develop synthesis methods providing a precise control of their size. At the moment, there are three main methods to synthesize metal clusters by soft chemical methods without templates: (1) the most established and studied one is the use of strong binding ligands (mainly thiols and phosphines) to inhibit the growth during the cluster formation, from which the initial proposed Brust–Schiffrin method[15] and the posterior multiple modifications warrant special mention.[16] Using such methods, in 2007, the group of R. Kornberg could synthesize very monodisperse Au_{102} clusters,[17] and resolved their structure by X-ray diffraction of a single crystal sample. Theoretical models allowed the understanding of the electronic structure and stability of this cluster, as well as other so-called magic clusters, which are clusters with a closed-shell configuration.[18] (2) Etching of very small nanoparticles with strong binding ligands was established by Nie's group in 2007,[19] based on previous works of cluster etching initiated by Wilcoxon.[20] (3) Kinetic control can be used for the synthesis of clusters even without surfactants and capping ligands.[21,22] Although not too much explored, this last method has the advantage that the un-protected clusters avoid the negative effect of ligands in catalytic applications, an area of large importance from both theoretical and application points of view. However, until now, only very small-unprotected clusters (below ≈ 6 atoms) could be synthesized by this method. One of the main reasons precluding the synthesis of larger clusters is the largely unknown underlying formation mechanisms, a matter which is also common – although to a lower extent – to the other synthetic methods mentioned above.[16] Therefore, studies contributing to the unraveling of such mechanisms are very important for the development of new scalable methods to produce monodisperse clusters of different materials.

Small metal clusters have been shown to be good catalysts for the formation of different anisotropic structures,[23] and seem to play an important role in the nucleation and growth of nanoparticles.[24] Here we demonstrate that small Cu_5 clusters can also be used as catalysts to control the formation of larger cysteine-capped $Cu_{\approx 10}$ clusters, which cannot be formed in the absence of the catalyst. The results clearly show that the small catalytic Cu_5 clusters not only prevent the formation of nanoparticles (mainly of copper oxides) or Cu(I)–cysteine complexes, but also may provide new insights into the intricate formation mechanisms of metal clusters. Finally, we show that the synthesized clusters display high catalytic efficiencies for the photocatalytic degradation of methyl orange by visible light.

[a] *Physical Chemistry Department, Faculty of Chemistry, and NANOMAG Laboratory, IMATUS, University of Santiago de Compostela, E-15782, Santiago de Compostela, Spain. E-mail: malopez.quintela@usc.es, buceta.david@gmail.com*

[b] *Instituto de Investigaciones Fisicoquímicas Teóricas y Aplicadas – INIFTA (CONICET, UNLP), 1900, La Plata, Argentina*

† Electronic supplementary information (ESI) available. CCDC. For ESI and crystallographic data in CIF or other electronic format see DOI: **https://doi.org/10.1039/d2cp04550h**

2. Experimental methods

2.1. Materials

Copper sheet (99%) and platinum sheet (99.95%) were purchased from Goodfellow. Alumina nanoparticles (average size ≈ 50 nm) and cloth pads were purchased from Buehler. 600 grit sandpaper was supplied by Wolfcraft. All water solutions were prepared with MilliQ grade water using a Direct-Q8UV system from Millipore. $CuNO_3$, L-Cysteine, $NaBH_4$, NaOH, $HClO_4$ and H_2SO_4 were purchased from Sigma-Aldrich.

2.2. Cu cluster synthesis

The first step was the synthesis of *naked* Cu_5 clusters (to be used as catalysts for the medium size cluster formation), *via* an electrochemical process previously reported.[22] Then, 1 mL of a freshly prepared Cu_5 sample (12 mg L^{-1}) was added to 500 mL of deoxygenated MiliQ water (bubbling N_2 for at least 45 min) and the Cu^{2+} ion concentration was adjusted to 25 mg L^{-1} with $CuNO_3$. To this solution 900 μL of L-Cysteine (50 mM) and 200 μL $NaBH_4$ (112 mM) were added and stirred for 1 h in a N_2 atmosphere followed by 12 h with no stirring. After this time, sample was characterized and stored at room temperature in an air atmosphere. The presence of ions in the final cluster samples was checked observing the presence/absence of precipitation after adding NaOH.

2.3. Cu cluster characterization

The cluster samples were characterized by UV-Vis and Fluorescence Spectroscopy, Atomic Force Microscopy and X-ray Absorption Spectroscopy.

Both UV-Vis and Fluorescence Spectroscopy were carried out at room temperature using 1 cm path-length Hellma quartz cuvettes. UV-vis spectra were recorded on a Thermo Evolution 300 UV-Visible spectrometer and fluorescence spectra were recorded using a Cary Eclipse Varian fluorimeter.

Atomic Force Microscopy (AFM) measurements were conducted under normal ambient conditions using a XE-100 instrument (Park Systems) in non-contact mode. The AFM tips were aluminum-coated silicon ACTA from Park Systems with a resonance frequency of 325 kHz. For AFM imaging, a drop of a diluted sample of Cu clusters was deposited onto a freshly cleaved mica sheet (SPI Supplies, Grade V-1 Muscovite), which was thoroughly washed with Milli-Q water and dried under nitrogen flow.

X-Ray Absorption Spectroscopy (XAS) measurements were performed at the XAFS2 beamline of the LNLS (Laboratorio Nacional de Luz Sincrotron), Campinas, Brazil. XANES and EXAFS spectra at the Cu K-edge (8979 eV) were recorded at room temperature using a Si (111) single channel-cut crystal monochromator. Cu–cysteine clusters in water solution were placed in a liquid cell with Kapton windows and measurements were performed in fluorescence mode using a 16-element Ge detector. In order to increase the signal-to-noise ratio, 6 scans were averaged. Cu references were measured in transmission mode with two ion chambers as detectors. XANES spectra normalization and EXAFS oscillation extraction and fitting were performed using the "IFEFFIT" software package.[25]

2.4. Photocatalytic activity

For the photocatalytic experiments two solutions were prepared: an aqueous solution of methyl orange (20.5×10^{-3} M, 8 μL) mixed with Cu-cys (1.25 mg L^{-1}, 3 mL) and a blank of methyl orange of the same final concentration (5.5×10^{-5} M, 3 mL). Samples were irradiated with a 60 W visible light bulb at 10 cm distance. The UV-Vis spectra of the solutions were recorded to follow up the reactions on a Hewlett-Packard 8452A Diode Array spectrophotometer (190–800 nm). When photooxidized by the Cu-cys, the MO was introduced again into the solution to study catalyst recyclability.

3. Results and discussion

Fig. 1a shows the UV-Vis spectrum of the Cu-capped cysteine clusters (Cu-cys) compared to that of *naked* Cu_5 clusters obtained before.[22] The Cu plasmon band (around 560 nm)[26] cannot be observed indicating the non-metallic character of the

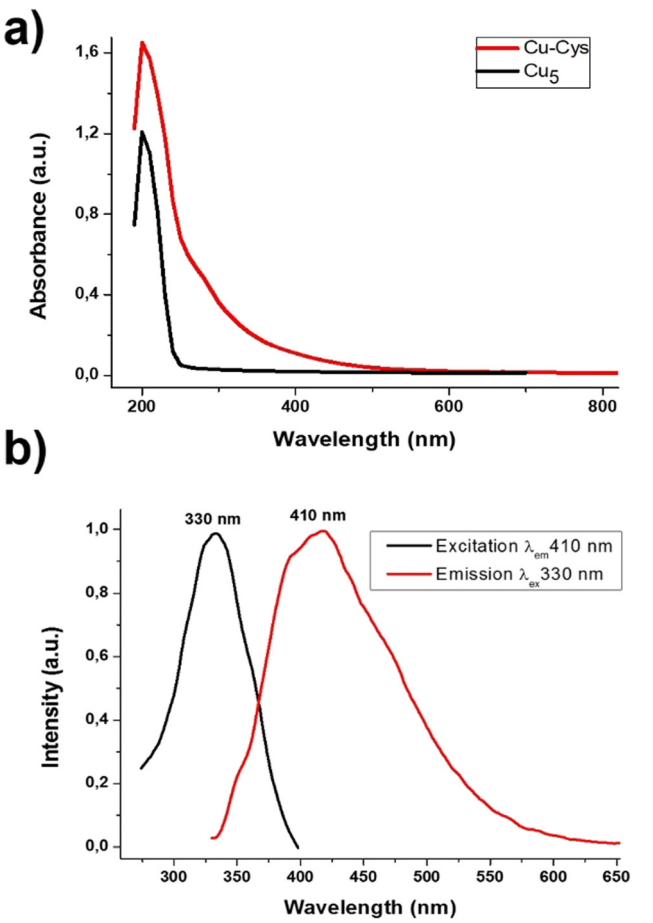

Fig. 1 (a) UV-Vis absorption spectrum of the Cu-cys sample and Cu_5 clusters (for comparison). (b) Photoluminescence spectra of the Cu-cys sample. Red line: emission spectrum at $\lambda_{excitation}$ = 330 nm; black line: excitation spectrum at $\lambda_{emission}$ = 410 nm.

Cu-cys clusters. Cu-cys shows an absorption band at higher wavelengths than Cu_5, and also a continuous decrease when increasing the wavelength, which reminds the absorption of medium size clusters, as we have reported before for Cu and Ag clusters.[27,28] This is the first indication that larger Cu clusters ($>Cu_5$) are produced.

Clusters are known to show florescence depending on their size, the emission wavelengths increasing with the cluster size.[29,30] The emission can be used to estimate the size of clusters by the simple quantum mechanical Jellium model,[31] which was developed for clusters in the gas phase,[32] and states in which $N = (E_F/E_{em})^3$, where N is the number of atoms of the cluster, E_F the kinetic Fermi energy of bulk metal ($E_F \approx 6.5$ eV, for Cu)[3] and E_{em} the cluster's emission energy (Note: in quantum dots, E_{em} is usually used to calculate the band gap, $E_g = E_{em}$, which can be also estimated from the absorption energy through the Tauc plot, but absorption cannot be used in clusters due to the presence of isomers with different absorption properties, but with only one preferred emission, see *e.g.* ref. 33). This equation describes accurately the size-dependent electronic structure and electronic transitions of small clusters, as was firstly demonstrated by R. M. Dickson[29,31] for Au clusters in dendrimers. Many other experimental[21,22,29,34,35] and theoretical calculations[18,31] show that this relationship between the emission and the number of atoms can be extended to Ag and Cu clusters (*i.e.* clusters of highly polarizable metals) protected by weak ligands. Such results suggest nearly spherical electronic cluster structures with electrons bound by an approximately harmonic potential, at least until $N \approx 20$ (see ref. 29 for details).

Fig. 1b shows the emission and excitation spectra of Cu-cys clusters, with the emission peak located at $E_{em} \approx 410$ nm ($\approx$3.0 eV). With this value, from the Jellium scaling law, one can deduce that the Cu-cys clusters would contain $\approx$10 atoms. It is interesting to note that there is an excitation dependent emission (EDE) with a red shift of around 40 nm (see Fig. 1 in ESI†). The simplest explanation for this red shift could be the presence of larger clusters in the approximate range of 10–14 atoms, but the presence of such large clusters can be disregarded by the EXAFS results, as we will show below. It must be noted that EDE has been reported in different nanoparticle materials.[36,37]

As for the other previously synthesized copper clusters,[22,28] non-contact AFM was used to calculate the average cluster size. Cu-cys clusters were deposited on mica substrates with an average roughness of 149 pm. The results can be seen in Fig. 2, indicating an average size of 1.2 $\pm$ 0.1 nm, which is in very good agreement with previously reported medium size Cu clusters.[28,38] This result also indicates that, contrary to Cu_5, this cluster has a 3D geometry, which is in agreement with the theoretical geometry predictions for Cu clusters with above $\approx$5 atoms.[39,40]

Fig. 3 shows the Cu-K XANES spectra of the Cu-cys sample in water and different Cu reference compounds and the Fourier Transform of the EXAFS oscillation of the Cu-cys sample as well as the corresponding fit (the obtained parameters are shown in Table 1). XANES is a powerful tool for chemically selective

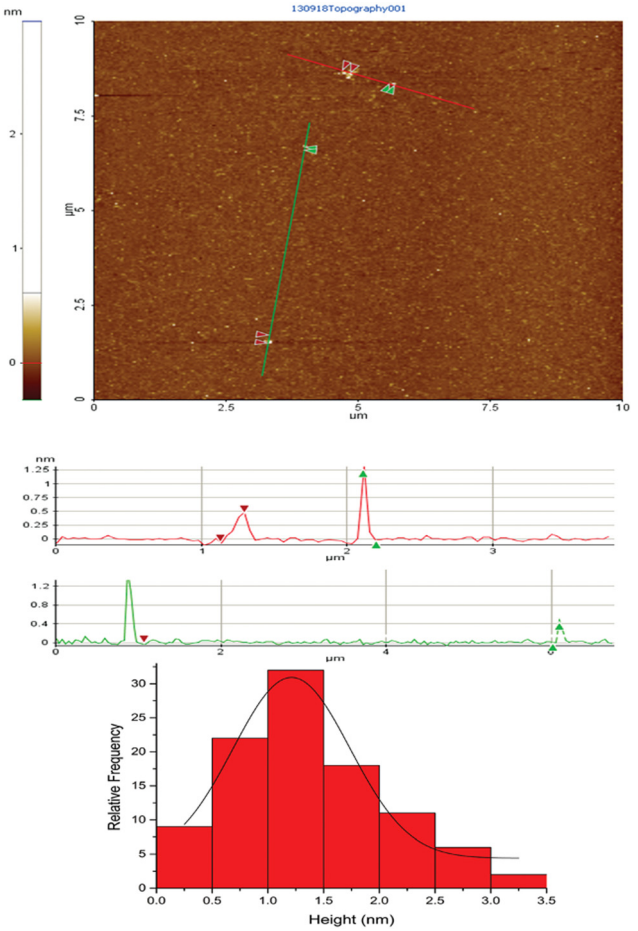

Fig. 2 AFM picture of Cu-cys deposited on mica (mean square roughness $\approx$ 149 pm) (up) and profiles throughout the red and green lines depicted on the AFM picture (down).

determination of the oxidation state and local symmetry of the absorbing atom while EXAFS provides information of the number, distance, and nature of the first neighbors of the absorbing atom. Therefore, these experiments were performed to precisely determine the average oxidation states of the Cys-capped Cu clusters and to help in the determination of their size.

As shown in Fig. 3, the energy edge shift of Cu-cys spectrum is null with respect to a metallic reference, which indicates that the sample has a majority presence of $Cu^{(0)}$. This can be also confirmed by EXAFS results, which show the existence of a Cu–Cu shell with the same interatomic distance of metallic Cu (see Table 1). Consistently, the nonappearance of species with Cu(I) or Cu(II) oxidation states in the XANES results implies the absence of Cu–cysteine complexes. In effect, different XANES features and average oxidation states, were already reported for $Cu/(C_{16}S)_2$, and the $Cu/(C_{18}S)_2$ crystals.[41] Additionally, Cu(I)[42,43] and Cu(II)–cysteine complexes,[44] prepared from $CuSO_4$ and L-cysteine hydrochloride according to the protocol outlined by Dokken *et al.*,[44] were already characterized as model compounds by XANES and EXAFS.

As mentioned before, the Cu–Cu fitted coordination shell (see Table 1) represents direct experimental evidence of the

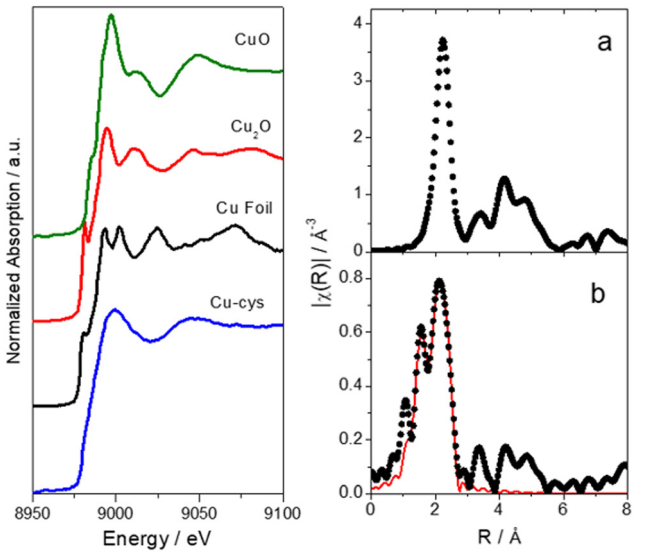

Fig. 3 Left: Cu-K XANES spectra of a Cu-cys sample in water and different reference compounds. Right: Fourier Transforms of the $k^2\chi$ ($Å^{-3}$) of (a) metallic Cu obtained from a Cu foil (black dots) and (b) Cu-sys sample (black dots). Solid red line corresponds to the fitted function (the parameters obtained from the fit are shown in Table 1). Note: distance is not phase corrected.

Table 1 Fitted Cu-K EXAFS parameters for Cu-cys sample. N is the average coordination number, R the interatomic distance and σ the Debye–Waller factor

Shell	N	R (Å)	σ^2 ($Å^2$)
Cu–N	0.9 ± 0.2	1.99 ± 0.03	0.003 ± 0.001
Cu–Cu	3.6 ± 0.8	2.55 ± 0.02	0.010 ± 0.002

formation of Cu clusters. The Cu–Cu fitted interatomic distance corresponds to the metallic Cu (2.5527 Å,[45]) and the small average coordination number of 3.6 would correspond, in principle, to a cluster with $< \approx 10$ atoms (a spherical-shaped cluster with 13 atoms would have a coordination number of 5.5).

In respect to the protecting agent of the Cu-cys clusters, EXAFS fitted parameters admit one type of linkage, *via* N interaction between the Cu atoms of the clusters and the cysteine molecules. Indeed, it has been reported that cysteine molecules could bind to the metal surface *via* –SH or $–NH_2$ linkage, as well as electrostatically *via* the carboxylic acid group in aqueous solution.[46,47] Cysteine can coordinate to the copper surface with more than one donor point forming most stable particles like metal chelates,[48] which is consistent with our EXAFS analysis. Additionally, the reported values for bond length in copper complexes of bidentate ligands containing nitrogen and sulfur donors are also in agreement with our experiments.[49]

With the described synthesis method one can produce up to roughly a gram of cysteine-capped $Cu_{\approx 10}$ (Cu-cys) clusters per day in an easy way. It has to be noticed that the amounts of clusters produced are of the order of the Cu ions present in the samples before reduction and are much higher (by around 3 orders of magnitude) than the used Cu_5 clusters, demonstrating that Cu_5 acts as a catalyst for the formation of the larger clusters. It is interesting to note that the synthesis only takes place when Cu_5 is present in the reaction media. When the reaction is performed under the same conditions without Cu_5 clusters, a mixture of different copper oxides was obtained (results not shown). These results clearly indicate that Cu_5 clusters should be directed and focused on in the reaction for the production of $Cu_{\approx 10}$ clusters. It was also found that the $[Cu_5]/[Cu\ ions]$ ratio (R) is critical ($R_{crit} \approx 0.005$) for the formation of such larger $Cu_{\approx 10}$ clusters, because when this ratio is diminished the formation of Cu(I)–cysteine complexes begins to compete with the formation of clusters. Fig. 4 shows a scheme summarizing all these results.

As we said above, although Brust–Schiffrin reactions have been extensively studied, the detailed reaction mechanisms are unknown, especially the precursor species present in solution before the reduction step. The results obtained here (see scheme) point to the idea that small catalytic clusters may be the precursor species needed for the formation of clusters in such methods, and that the precise control of the concentration of such catalytic clusters is pivotal for the cluster synthesis, opening new possibilities for understanding and exploring novel and more efficient cluster production methods.

Cu-cys clusters remain stable for more than 1 year at room temperature with no appreciable changes in their optical properties (see Fig. 5). In order to further examine the Cu-cys cluster stability we performed several experiments against temperature (up to 60 °C for 24 h), pH (between 3 and 14) and photobleaching experiments (irradiation at 220 nm for 24 h) (see ESI,† Fig. S2–S4). As previously observed with other Cu clusters,[22,28] no changes were detected, thus making clear the great stability of the synthesized Cu-cys clusters, especially compared to bulk copper or Cu nanoparticles. This high stability can be associated with the position of the HOMO level ($-(\Phi_{Cu} + \frac{1}{2} E_g) \approx -(4.7 + 1.5) = -6.2$ eV with respect to the vacuum level *i.e.* $\approx +1.7$ V RHE; being Φ_C the work function of bulk Cu, and using $E_g = E_{em}$), indicating that the oxidation of such Cu clusters is extremely difficult, as was previously reported.[22,28]

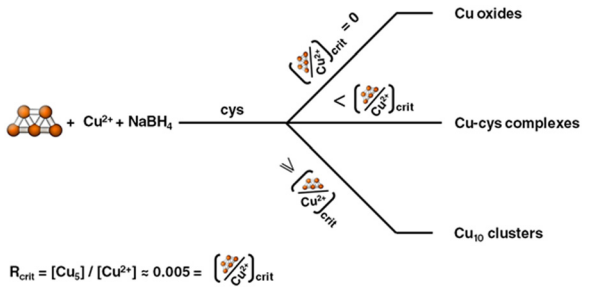

Fig. 4 Scheme representing the products obtained after reaction of $CuNO_3$, cysteine and $NaBH_4$ using different amounts of catalytic Cu_5 clusters.

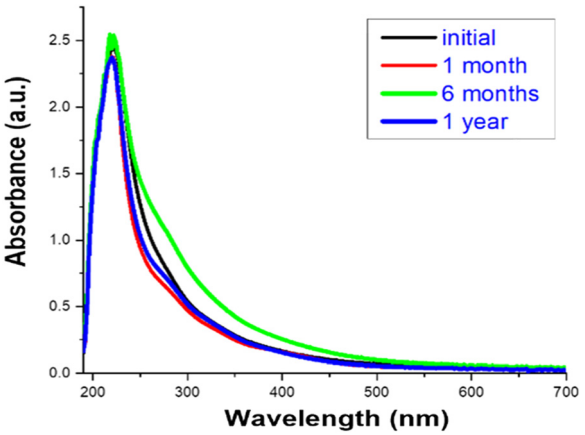

Fig. 5 UV-Vis spectrum of a Cu-cys sample in water stored at RT for one year.

The photocatalytic activity of metal clusters is already known.[8,10,50,51] Very small clusters with large bandgaps show activity in the UV range while larger size clusters, with smaller bandgaps, show activity in the visible range. It was previously shown that Cu clusters, due to their atomic size, are very efficient photooxidants because the oxidation seems to be carried out directly by the photogenerated holes, in contrast to classical semiconductors.[52] Taking this into account we explore the use of Cu-cys clusters for the photooxidation of methyl orange (a dye used as a contaminant model). The results shown in Fig. 6 are very exciting. With a normal visible light bulb of 60 W, 1.25 mg L^{-1} of Cu-cys clusters degrade 0.018 g L^{-1} (5.5×10^{-5} M) of MO in 120 min, which implies a TOR of 7.2 h^{-1} (the evolution of the photodegradation process can be seen in the ESI,† Fig. S5, as well as the corresponding exponential fitting, Fig. S6 (ESI†), giving a rate constant = 0.03 min^{-1}). Moreover, this photocatalytic activity is maintained for, at least, four continuous additions of MO. For comparison purposes, using a 400 W high pressure mercury vapor lamp, 2 g L^{-1} of N/Mn co-doped TiO_2 nanoparticles degrade 5 mg L^{-1} of MO in 90 min,[53] which implies a TOR of 1.7×10^{-3} h^{-1}, and using a 400 W Osram lamp; 1g L^{-1} of Cu/S-codoped TiO_2 nanoparticles degrade 10 mg L^{-1} of MO in 240 min,[54] which results in a TOR of 2.5×10^{-3} h^{-1}. A more recent study using ZnO assisted with Ag metal plasmons[55] shows that, even with such new strategies, the obtained TOR is $\approx 10^{-3}$ h^{-1}. We can see that the TOR using clusters is $\approx$3 orders of magnitude larger than the one using common semiconductors, which further support the idea that the photooxidation mechanism with clusters is much more efficient, probably since each cluster works as a very localized ($\approx$1 nm) photocatalytic center and the produced hole is highly oxidant ($\approx$+1.7 V RHE). This clearly demonstrates the potential of medium size copper clusters to act as highly efficient photocatalysts in the visible range. Their characteristics of being highly stable, cheap, and now easy to synthetize in the range of grams/day, put them in the lead of possible common SC relief, but also open new opportunities for applications in catalysis.

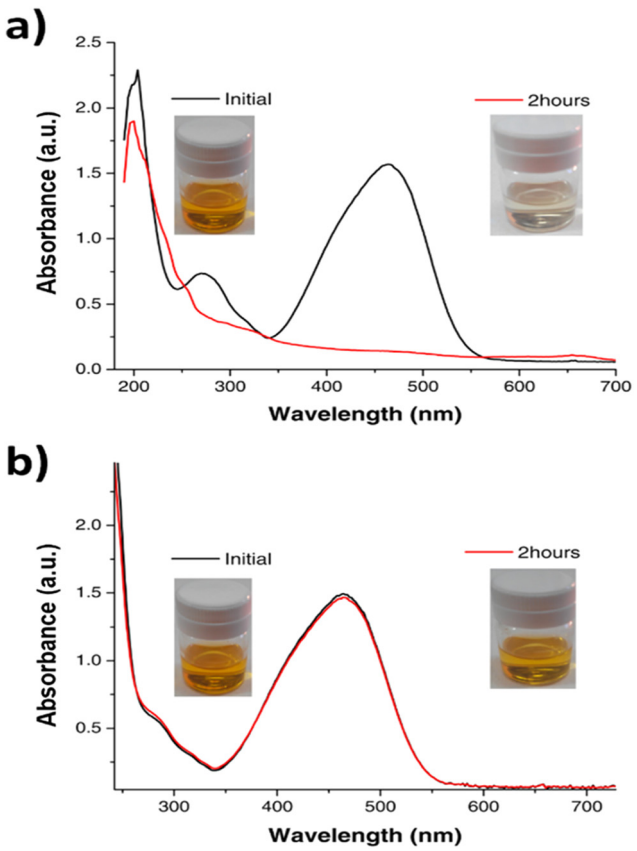

Fig. 6 (a) UV-Vis absorption spectrum of MO solution with Cu-cys clusters before and after irradiation with visible light during two hours. Pictures represent the sample color before and after irradiation. (b) UV-Vis absorption spectrum of MO blank solution before and after irradiation with visible light during two hours. Pictures represent the sample color before and after irradiation.

4. Conclusions

We have shown that small Cu_5 clusters can be conveniently used to direct and focus the formation of larger $Cu_{\approx 10}$ clusters when Cu(II) is reduced with $NaBH_4$ using cysteine as a capping agent. The concentration of Cu_5 clusters is critical ($R_{crit} = [Cu_5]_{crit}/[Cu\ ions] \approx 0.005$) for the synthesis of cysteine-capped $Cu_{\approx 10}$ clusters, because for small ratios a competing reaction with the formation of Cu(I)–cysteine complexes is favored. These results point to the idea that catalytic small clusters could be plausible candidates for the unknown precursor species present in solution before the reduction step, which are involved in the different methods developed for the synthesis of clusters. Finally, the synthesized medium size cysteine-capped $Cu_{\approx 10}$ clusters show excellent photocatalytic activities for the decomposition of MO using a very low power visible light.

Author contributions

Shahana Huseyinova (sahanehuseynova@gmail.com) and José M. Blanco Trillo (blanco.josemanuel@outlook.es) contributed equally (as co-first authors) to this work.

Conflicts of interest

There are no conflicts of interest to declare.

Acknowledgements

This research was partially supported by the Consellería de Educación (Xunta de Galicia), Grants No. Grupos Ref. Comp. ED431C 2021/16, the European Union's Horizon 2020 Research and Innovation Programme (Bac-To-Fuel) under Grant Agreement No. 825999; ANPCyT PICT (2017-1220 and 2017-3944) and UNLP (Project 11/X937), Argentina. This research used resources of the Brazilian Synchrotron Light Laboratory (LNLS), an open national facility operated by the Brazilian Centre for Research in Energy and Materials (CNPEM) for the Brazilian Ministry for Science, Technology, Innovations and Communications (MCTIC). The XAFS2 beamline staff is acknowledged for the assistance during the experiments (proposals 20160754 and 20170907)

References

1 X. Wu, X. He, K. Wang, C. Xie, B. Zhou and Z. Qing, Ultrasmall near-infrared gold nanoclusters for tumor fluorescence imaging in vivo, *Nanoscale*, 2010, **2**, 2244–2249.
2 M. J. Barthel, I. Angeloni, A. Petrelli, T. Avellini, A. Scarpellini, G. Bertoni, A. Armirotti, I. Moreels and T. Pellegrino, Synthesis of Highly Fluorescent Copper Clusters Using Living Polymer Chains as Combined Reducing Agents and Ligands, *ACS Nano*, 2015, **9**, 11886–11897.
3 N. Vilar-Vidal, J. Rivas and M. A. López-Quintela, Size dependent catalytic activity of reusable subnanometer copper(0) clusters, *ACS Catal.*, 2012, **2**, 1693–1697.
4 Y. Liu, H. Tsunoyama, T. Akita, S. Xie and T. Tsukuda, Aerobic Oxidation of Cyclohexane Catalyzed by Size-Controlled Au, *ACS Catal.*, 2011, **1**, 2–6.
5 Y. Chen, S. Ji, C. Chen, Q. Peng, D. Wang and Y. Li, Single-Atom Catalysts: Synthetic Strategies and Electrochemical Applications, *Joule*, 2018, **2**, 1242–1264.
6 P. Jena and Q. Sun, *Chem. Rev.*, 2018, **118**, 5755–5870.
7 T. Tsukuda and H. Häkkinen, ed., *Protected Metal Clusters: From Fundamentals to Applications*, Elsevier, Amsterdam, 2015.
8 R. Jin, C. Zeng, M. Zhou and Y. Chen, *Chem. Rev.*, 2016, **116**, 10346–10413.
9 E. C. Tyo and S. Vajda, Catalysis by clusters with precise numbers of atoms, *Nat. Nano*, 2015, **10**, 577–588.
10 L. Liu and A. Corma, *Chem. Rev.*, 2018, **118**, 4981–5079.
11 H. Chen, Z. Li, Z. Qin, H. J. Kim, H. Abroshan and G. Li, Silica-Encapsulated Gold Nanoclusters for Efficient Acetylene Hydrogenation to Ethylene, *ACS Appl. Nano Mater.*, 2019, **2**, 2999–3006.
12 M. A. Abbas, T.-Y. Kim, S. U. Lee, Y. S. Kang and J. H. Bang, Exploring Interfacial Events in Gold-Nanocluster-Sensitized Solar Cells: Insights into the Effects of the Cluster Size and Electrolyte on Solar Cell Performance, *J. Am. Chem. Soc.*, 2016, **138**, 390–401.
13 F. X. Xiao, S. F. Hung, J. Miao, H. Y. Wang, H. Yang and B. Liu, Metal-Cluster-Decorated TiO2 Nanotube Arrays: A Composite Heterostructure toward Versatile Photocatalytic and Photoelectrochemical Applications, *Small*, 2015, **11**, 554–567.
14 N. Sakai and T. Tatsuma, Photovoltaic Properties of Glutathione-Protected Gold Clusters Adsorbed on TiO2 Electrodes, *Adv. Mater.*, 2010, **22**, 3185–3188.
15 M. Brust, M. Walker, D. Bethell, D. J. Schiffrin and R. Whyman, Synthesis of thiol-derivatised gold nanoparticles in a two-phase Liquid–Liquid system, *J. Chem. Soc., Chem. Commun.*, 1994, **0**, 801–802.
16 Y. Lu and W. Chen, CRITICAL REVIEW Chemical Society Reviews Sub-nanometre sized metal clusters: from synthetic challenges to the unique property discoveries, *Chem. Soc. Rev.*, 2012, **41**, 3594–3623.
17 P. D. Jadzinsky, G. Calero, C. J. Ackerson, D. A. Bushnell and R. D. Kornberg, Structure of a thiol monolayer-protected gold nanoparticle at 1.1 Å resolution, *Science*, 2007, **318**, 430–433.
18 M. Walter, J. Akola, O. Lopez-Acevedo, P. D. Jadzinsky, G. Calero, C. J. Ackerson, R. L. Whetten, H. Grönbeck and H. Häkkinen, A unified view of ligand-protected gold clusters as superatom complexes, *Proc. Natl. Acad. Sci. U. S. A.*, 2008, **105**, 9157–9162.
19 H. Duan and S. Nie, Etching Colloidal Gold Nanocrystals with Hyperbranched and Multivalent Polymers: A New Route to Fluorescent and Water-Soluble Atomic Clusters, *J. Am. Chem. Soc.*, 2007, **129**, 2412–2413.
20 J. P. Wilcoxon and P. Provencio, Etching and Aging Effects in Nanosize Au Clusters Investigated Using High-Resolution Size-Exclusion Chromatography, *J. Phys. Chem. B*, 2003, **107**, 12949–12957.
21 D. Buceta, N. Busto, G. Barone, J. M. J. M. Leal, F. Domínguez, L. J. L. J. Giovanetti, F. G. F. G. Requejo, B. García, M. A. López-Quintela and M. A. Lõpez-Quintela, Ag2 and Ag3 Clusters: Synthesis, Characterization, and Interaction with DNA, *Angew. Chem., Int. Ed.*, 2015, **54**, 7612–7616.
22 S. Huseyinova, J. Blanco, G. Requejo, J. M. Ramallo-López, M. C. Blanco, D. Buceta and M. A. López-Quintela, Synthesis of Highly Stable Surfactant-free Cu 5 Clusters in Water, *J. Phys. Chem. C*, 2016, **120**, 15902–15908.
23 Y. A. Attia, D. Buceta, C. Blanco-Varela, M. B. Mohamed, G. Barone and M. A. López-Quintela, Structure-directing and high-efficiency photocatalytic hydrogen production by Ag clusters, *J. Am. Chem. Soc.*, 2014, **136**, 1182–1185.
24 Y. Piñeiro, D. Buceta, J. Calvo, S. Huseyinova, M. Cuerva, Á. Pérez, B. Domínguez and M. A. López-quintela, Large stability and high catalytic activities of sub-nm metal (0) clusters: Implications into the nucleation and growth theory, *J. Colloid Interface Sci.*, 2015, **449**, 279–285.
25 B. Ravel and M. Newville, ATHENA, ARTEMIS, HEPHAESTUS: data analysis for X-ray absorption spectroscopy using IFEFFIT, *J. Synchrotron Radiat.*, 2005, **12**, 537–541.
26 I. Lisiecki, M. P. Pileni and C. E. N. Saclay, Copper Metallic Particles Synthesized 'in Situ' in Reverse Micelles: Influence of Various Parameters on the Size of the Particles, *J. Phys. Chem.*, 1995, **99**, 5077–5082.

27 B. S. González, M. C. Blanco and M. A. López-Quintela, Single step electrochemical synthesis of hydrophilic/hydrophobic Ag5 and Ag6 blue luminescent clusters, *Nanoscale*, 2012, **4**, 7632–7635.
28 N. Vilar-Vidal, M. C. Blanco, M. A. López-Quintela, J. Rivas and C. Serra, Electrochemical synthesis of very stable photoluminescent copper clusters, *J. Phys. Chem. C*, 2010, **114**, 15924–15930.
29 J. Zheng, P. R. Nicovich and R. M. Dickson, Highly fluorescent noble-metal quantum dots, *Annu. Rev. Phys. Chem.*, 2007, **58**, 409–431.
30 M. A. López Quintela and B. Santiago-Gónzalez, New Strategies and Synthetic Routes to Synthesize Fluorescent Atomic Quantum Clusters. in *Functional Nanometer-Sized Clusters of Transition Metals: Synthesis, Properties, and Applications*, Royal Society of Chemistry, Cambridge, 2014, 25–50.
31 J. Zheng, C. Zhang and R. M. Dickson, Highly fluorescent, water-soluble, size-tunable gold quantum dots, *Phys. Rev. Lett.*, 2004, **93**, 077402.
32 D. M. Wood and N. W. Ashcroft, Quantum size effects in the optical properties of small metallic particles, *Phys. Rev. B: Condens. Matter Mater. Phys.*, 1982, **25**, 6255–6274.
33 C. Sieber, J. Buttet, W. Harbich, C. Félix, R. Mitrić and V. Bonačić-Koutecký, Isomer-specific spectroscopy of metal clusters trapped in a matrix: [Formula Presented], *Phys. Rev. A: At., Mol., Opt. Phys.*, 2004, **70**, 4.
34 V. Porto, E. Borrajo, D. Buceta, C. Carneiro, S. Huseyinova, B. Domínguez, K. J. E. Borgman, M. Lakadamyali, M. F. Garcia-Parajo, J. Neissa, T. García-Caballero, G. Barone, M. C. Blanco, N. Busto, B. García, J. M. Leal, J. Blanco, J. Rivas, M. A. López-Quintela and F. Domínguez, Silver Atomic Quantum Clusters of Three Atoms for Cancer Therapy: Targeting Chromatin Compaction to Increase the Therapeutic Index of Chemotherapy, *Adv. Mater.*, 2018, **30**, 1801317.
35 V. Porto, D. Buceta, B. Dominguez, C. Carneiro, E. Borrajo, M. Fraile, N. Dávila-Ferreira, I. R. Arias, J. M. Blanco, J. M. Devida, L. J. Giovanetti, F. G. Requejo, J. C. Hernández, J. J. Calvino, M. López-Haro, G. Barone, A. M. James, T. García-Caballero, D. M. González-Castaño, M. Treder, W. Huber, A. Vidal, M. P. Murphy, M. A. López-Quintela and F. Domínguez, Low Atomicity Silver Clusters as Highly Selective Antitumoral Agents Through Irreversible Oxidation of Thiols, *Adv. Funct. Mater.*, 2022, 2113028.
36 K. M. Lee, W. Y. Cheng, C. Y. Chen, J. J. Shyue, C. C. Nieh, C. F. Chou, J. R. Lee, Y. Y. Lee, C. Y. Cheng, S. Y. Chang, T. C. Yang, M. C. Cheng and B. Y. Lin, Excitation-dependent visible fluorescence in decameric nanoparticles with monoacylglycerol cluster chromophores, *Nat. Commun.*, 2013, **4**, 1544.
37 S. K. Cushing, M. Li, F. Huang and N. Wu, Origin of Strong Excitation Wavelength Dependent Fluorescence of Graphene Oxide, *ACS Nano*, 2014, **8**, 1002–1013.
38 C. Vázquez-Vázquez, M. Bañobre-López, A. Mitra, M. A. López-Quintela and J. Rivas, Synthesis of Small Atomic Copper Clusters in Microemulsions, *Langmuir*, 2009, **25**, 8208–8216.
39 P. Calaminici, A. M. Köster and N. Russo, A density functional study of small copper clusters: Cun (n $\leqslant$5), *J. Chem. Phys.*, 1996, **105**, 9546.
40 P. Jaque and A. Toro-Labbé, Characterization of copper clusters through the use of density functional theory reactivity descriptors, *J. Chem. Phys.*, 2002, **117**, 3208–3218.
41 T.-Y. Chen, S.-F. Chen, H.-S. Sheu and C.-S. Yeh, Reactivity of Laser-Prepared Copper Nanoparticles: Oxidation of Thiols to Disulfides, *J. Phys. Chem. B*, 2002, **106**, 9717–9722.
42 B. M. Ryan, J. K. Kirby, F. Degryse, H. Harris, M. J. McLaughlin and K. Scheiderich, Copper speciation and isotopic fractionation in plants: uptake and translocation mechanisms, *New Phytol.*, 2013, **199**, 367–378.
43 M. J. Ceko, J. B. Aitken and H. H. Harris, Speciation of copper in a range of food types by X-ray absorption spectroscopy, *Food Chem.*, 2014, **164**, 50–54.
44 K. M. Dokken, J. G. Parsons, J. McClure and J. L. Gardea-Torresdey, Synthesis and structural analysis of copper(II) cysteine complexes, *Inorg. Chim. Acta*, 2009, **362**, 395–401.
45 R. W. G. Wyckoff, *Crystal Structures*, John Wiley Inderscience Publishers, 1969.
46 S. Mandal, A. Gole, N. Lala, R. Gonnade, V. Ganvir and M. Sastry, Studies on the Reversible Aggregation of Cysteine-Capped Colloidal Silver Particles Interconnected via Hydrogen Bonds, *Langmuir*, 2001, **17**, 6262–6268.
47 S. Aryal, B. K. C. Remant, N. Dharmaraj, N. Bhattarai, C. H. Kim and H. Y. Kim, Spectroscopic identification of SAu interaction in cysteine capped gold nanoparticles, *Spectrochim. Acta, Part A*, 2006, **63**, 160–163.
48 E. Fernández and M. Boronat, *J. Phys.: Condens. Matter*, 2019, **31**, 013002.
49 M. R. Malachowski, M. E. Adams, D. Murray, R. White, N. Elia, A. L. Rheingold, L. N. Zakharov and R. S. Kelly, Copper(II) complexes of bidentate ligands containing nitrogen and sulfur donors: Synthesis, structures, electrochemistry and catalytic properties, *Inorg. Chim. Acta*, 2009, **362**, 1247–1252.
50 H. Zhu, N. Goswami, Q. Yao, T. Chen, Y. Liu, Q. Xu, D. Chen, J. Lu and J. Xie, Cyclodextrin–gold nanocluster decorated TiO2 enhances photocatalytic decomposition of organic pollutants, *J. Mater. Chem. A*, 2018, **6**, 1102–1108.
51 J. González-Rodríguez, L. Fernández, Y. B. Bava, D. Buceta, C. Vázquez-Vázquez, M. A. López-Quintela, G. Feijoo and M. T. Moreira, Enhanced photocatalytic activity of semiconductor nanocomposites doped with Ag nanoclusters under UV and visible light, *Catalysts*, 2020, **10**, 1–10.
52 N. Vilar-vidal, J. R. Rey and M. A. L. Quintela, Green Emitter Copper Clusters as Highly Efficient and Reusable Visible Degradation Photocatalysts, *Small*, 2014, 3632–3636.
53 S. Thota, S. R. Tirukkovalluri and S. Bojja, Visible Light Induced Photocatalytic Degradation of Methyl Red with Codoped Titania, *J. Catal.*, 2014, **2014**, 1–7.
54 M. Hamadanian, A. Reisi-Vanani and A. Majedi, Synthesis, characterization and effect of calcination temperature on phase transformation and photocatalytic activity of Cu,S-codoped TiO2 nanoparticles, *Appl. Surf. Sci.*, 2010, **256**, 1837–1844.
55 V. E. Podasca and M. D. Damaceanu, ZnO-Ag based polymer composites as photocatalysts for highly efficient visible-light degradation of Methyl Orange, *J. Photochem. Photobiol., A*, 2021, **406**, 113003.